Supporting Information

Determination of the Structure and Geometry of N-Heterocyclic Carbenes on Au(111) using High-Resolution Spectroscopy

Giacomo Lovat,[a] Evan A. Doud,[b] Deyu Lu,[c] Gregor Kladnik,[de] Michael S. Inkpen,[a] Michael L. Steigerwald,[b] Dean Cvetko,[def] Mark S. Hybertsen,[c] Alberto Morgante,*[dg] Xavier Roy,*[b] Latha Venkataraman,*[ab]

[a] Department of Applied Physics and Applied Mathematics, Columbia University, New York
[b] Department of Chemistry, Columbia University, New York
[c] Center for Functional Nanomaterials, Brookhaven National Laboratory, Upton, New York
[d] CNR-IOM Laboratorio Nazionale TASC, Basovizza SS-14, km 163.5, 34012 Trieste, Italy
[e] Faculty of Mathematics and Physics, University of Ljubljana, Jadranska 19, Ljubljana, Slovenia
[f] J. Stefan Institute, Jamova 39, SI-1000, Ljubljana, Slovenia
[g] Department of Physics, University of Trieste, via A. Valerio 2, 34127, Trieste, Italy

1. Synthesis

General Information

2-Iodopropane was purchased from Acros Organics. CD_2Cl_2, CD_3OD, and D_2O were purchased from Cambridge Isotope. Tetrahydrofuran (THF) was purchased from Fisher Scientific. 1,3-Bis(2,6-diisopropylphenyl)-1,3-dihydro-2H-imidazol-2-ylidene, 1H-benzimidazole and K_2CO_3 were purchased from Sigma-Aldrich. 1,3-Dimethylimidazolium chloride was purchased from TCI Chemicals. 1,3-Diisopropylbenzimidazolium iodide was synthesized following literature procedures.[1] All reactions were carried out under inert atmosphere in a N_2-filled glovebox, unless otherwise noted.

1,3-dimethylimidazolium-2-carboxylate (NHC^{Me}–CO_2)

In a N_2 filled glovebox, 1,3-dimethylimidazolium chloride (198 mg, 1.5 mmol) and potassium *tert*-butoxide (255 mg, 2.2 mmol) were suspended in 20 mL THF in a 20 mL scintillation vial. The suspension was stirred for 1 hour at room temperature and then filtered through a 0.2 μm PTFE syringe filter into a Schlenk flask equipped with a stir bar. The Schlenk flask containing the reaction mixture was sealed with a rubber septum. The flask was removed from the glove box and connected to a Schlenk line. CO_2 was bubbled through the solution for 30 min. The precipitated solid was collected via filtration through a medium porosity frit, washed with THF (3 x 20 mL), and dried *in vacuo*. NHC^{Me}–CO_2 was obtained as a white solid. (Yield: 110 mg, 53%). Spectroscopic characterization data matched with previous reported data.[2]

1,3-diisopropylbenzimidazolium-2-carboxylate ($^{B}NHC^{iPr}$–CO_2)

$^{B}NHC^{iPr}$–CO_2 was synthesized following the same procedure as NHC^{Me}–CO_2, starting from 1,3-diisopropylbenzimidazolium iodide (500 mg, 1.5 mmol). $^{B}NHC^{iPr}$–CO_2 was obtained as a white solid. (Yield: 167 mg, 45%). Spectroscopic characterization data matched with previous reported data.[3]

1,3-bis(2,6-diisopropylphenyl)imidazolium-2-carboxylate (NHC^{dipp}–CO_2)

NHC^{dipp}–CO_2 was synthesized following the same procedure as NHC^{Me}–CO_2, starting from 1,3-bis(2,6-diisopropylphenyl)-1,3-dihydro-2H-imidazol-2-ylidene (100 mg, 250 μmol) and omitting the initial deprotonation step. NHC^{dipp}–CO_2 was obtained as a white solid (Yield: 31 mg, 28%) Spectroscopic characterization data matched with previous reported data.[4]

2. Sample Preparation

The NHC monolayers were prepared and characterized *in situ* at the ALOISA beamline of the Elettra synchrotron light laboratory (Trieste, Italy). Monolayers were deposited in a preparation chamber (base pressure $< 2 \times 10^{-9}$ mbar) by first cleaning the Au(111) single crystal by repeated cycles of Ar^+ sputtering and thermal annealing to 800 K. Cleanliness was checked by ensuring no O, N, and C signal in XPS. The compounds were sublimed onto the Au(111) surface using a Pyrex cell connected to the preparation chamber through a leak valve. The cell was gently heated to ~70 °C for 4 - 5 minutes to keep a constant NHC pressure in the chamber of about 10^{-7} mbar. The substrate was kept at -20 to -30 °C to grow the monolayer phase. Measurements were carried out in an experimental chamber with base pressure $< 2 \times 10^{-10}$ mbar.

3. Details of XPS and NEXAFS Measurements

X-ray photoemission spectroscopy (XPS) measurements were performed at the ALOISA beamline with the x-ray beam at grazing incidence (4°) to the sample surface. Photoelectrons from the sample were collected at an emission angle normal to the surface using a hemispherical electron analyzer with an acceptance angle of 2°, and an overall energy resolution of ~0.2 eV. The energy scale for XPS spectra was calibrated by aligning the Au $4f_{7/2}$ peak to a binding energy of 84.00 eV.

Near edge X-ray absorption fine-structure (NEXAFS) measurements were performed on the N and C K-edge by sweeping the incident photon energy from 394 to 413 eV and from 278 to 310 eV, respectively. The photon incidence angle was set to 6°. Spectra were acquired using a Channeltron detector with a wide acceptance angle in the partial electron yield mode. The photon

flux was monitored on the last optical element along the beam path. The sample normal was oriented either parallel (*p*-pol) or perpendicular (*s*-pol) to the light polarization.

The relative intensity of the nitrogen NEXAFS signal in *p*-pol and *s*-pol for the N 1s to LUMO transition was used for estimating the orientation of the carbene ring relative to the surface plane, whereas the orientation of the aryl groups for NHC^{dipp} was determined with the polarization-dependent signal of the C1s NEXAFS. The molecular tilt angle θ is estimated relative to the surface plane using the formula: $\tan(\theta) = \sqrt{2I_s/I_p}$, where I_s and I_p are the intensities of the π*-LUMO NEXAFS peak from the *s*-pol and *p*-pol spectra, respectively.[5]

4. Details of DFT Calculations

The PWSCF software in the Quantum Espresso package was used to simulate the adsorption of the NHCs on an Au(111) slab.[6] The "optB88-vdW" exchange and correlation functional was used for all calculations as it has been demonstrated to provide a good description of dispersion interactions. All structures were relaxed until interatomic forces in the self-consistent calculation were smaller than 0.026 eV/Å and energy variations smaller than 10^{-5} Ry. Adsorption relaxations were performed using an Au(111) 4-layer slab. The two bottom layers were held fixed while the top two ones were relaxed. The slab size was 3×3, 4×4 and 5×5 unit cells for NHC^{Me}, $^{B}NHC^{iPr}$, and NHC^{dipp}, respectively, whereas slabs of size 5×4 and 5×7 unit cells were used for the NHC^{Me}–Au^{ad}–NHC^{Me} and $^{B}NHC^{iPr}$–Au^{ad}–$^{B}NHC^{iPr}$ complexes. The Au adatom was relaxed on a hollow position of the Au(111) surface slab prior to optimizing the adatom-adsorbed NHC systems. Convergence of the calculations relative to the cell size was also tested. The adsorption energies were calculated as follows by subtracting the sum of the energies of the separately relaxed molecule and slab systems from the total energy. All illustrations of ball-and-stick adsorption models were produced using VESTA 3 software.[6]

5. Additional Experimental and Theoretical Data

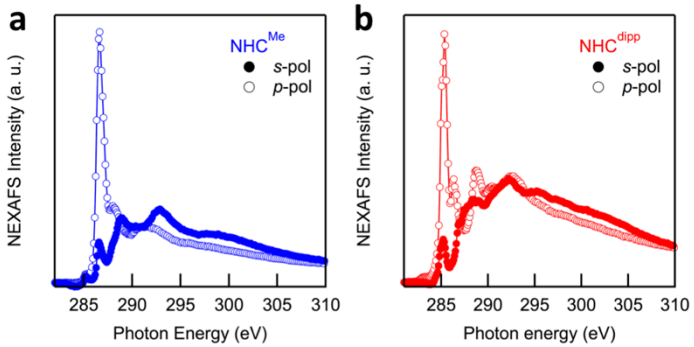

Figure S1: NEXAFS spectra collected at the C K-edge of (a) NHC^{Me} monolayer and (b) NHC^{dipp} in *s*-pol (filled markers) and *p*-pol (empty markers). The first 1s to LUMO resonance corresponds to a π* orbital localized on the NHC ring (E_{photon} = 286.6 eV) in NHC^{Me} and to π* orbital localized on the aryl substituents (E_{photon} = 285.3 eV) in NHC^{dipp}. The second resonance in NHC^{dipp} is the π* orbital localized on the NHC ring (E_{photon} = 286.3 eV). Using the polarization-dependent data for NHC^{dipp}, we determine that the angle of the aryl substituent plane relative to the Au surface plane is ~29°.

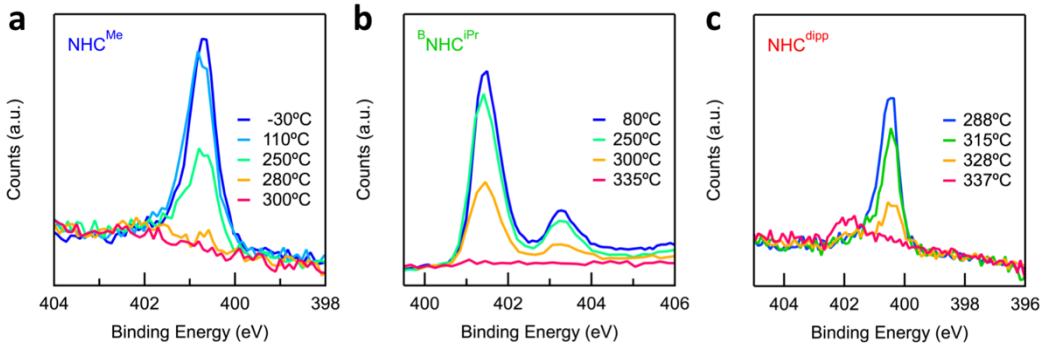

Figure S2: N 1s XPS spectra collected at different temperatures for (a) NHC^{Me}, (b) $^{B}NHC^{iPr}$, and (c) NHC^{dipp} monolayers. All NHCs exhibit similar desorption temperatures at ~280-330 ºC.

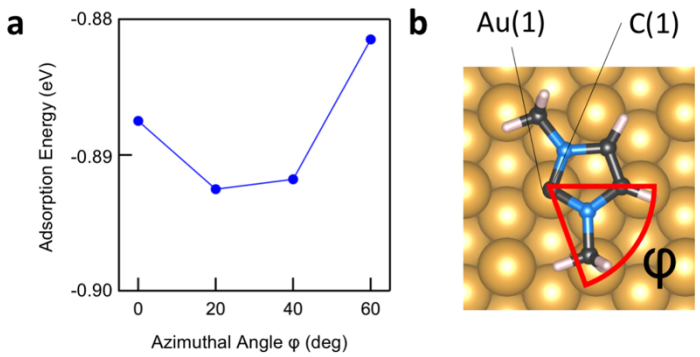

Figure S3: (a) Adsorption energy as a function of the azimuthal angle φ for NHC^{Me} adsorbed in a flat adsorption geometry on a 3×3 Au slab. NHC^{Me} carbenic carbon atom C(1) lies atop an Au(111) surface atom, Au(1). The angle of rotation of the molecule about the axis normal to the surface plane defined by C(1) and Au(1) and indicated by the arrow. The variation of adsorption energy as the molecule is rotated is ~0.01 eV. (b) Modeled structure of NHC^{Me} on a 3×3 Au slab used to calculate the adsorption energy as a function of azimuthal angle.

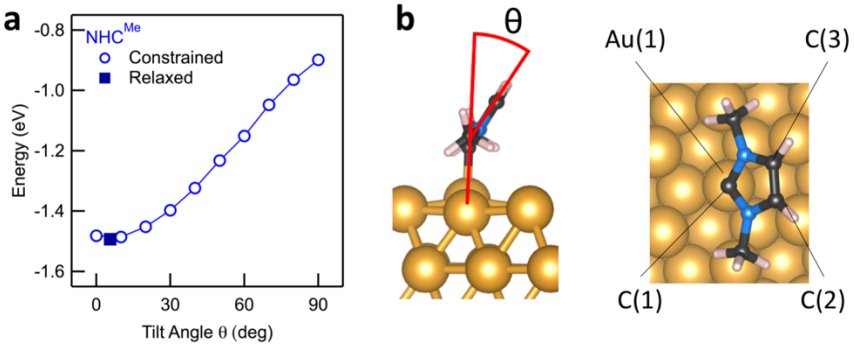

Figure S4: (a) Adsorption energy as a function of tilt angle θ for NHC^{Me} adsorbed on a 3×3 Au slab. The hollow blue circles are the adsorption energies calculated with two constraints: the angles defined by Au(1)-C(1)-C(2) and Au(1)-C(1)-C(3) are kept fixed during optimization. This ensures that θ remains fixed to a chosen value. A steep increase in adsorption energy is observed as θ increases. The solid square data point is obtained after lifting all constraints (starting from θ = 30º); the adsorption energy is –1.49 eV at θ ~15º. (b) Modeled structure of NHC^{Me} on a 3×3 Au slab used to calculate the adsorption energy as a function of tilt angle.

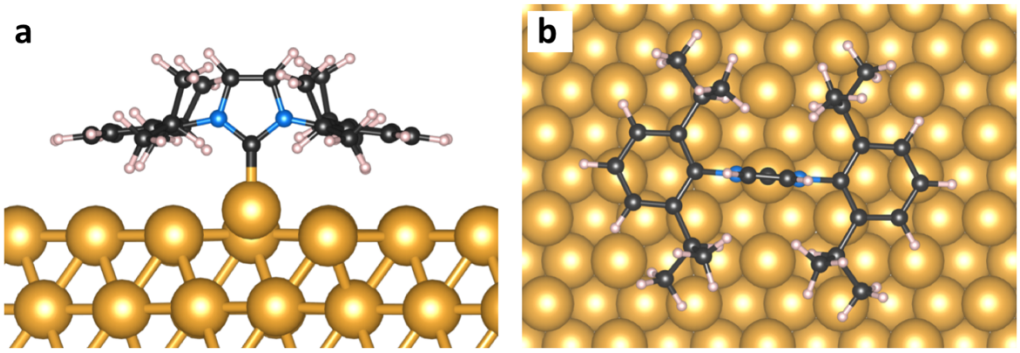

Figure S5: DFT-optimized energy minimum structure of NHC^{dipp} on a 5×5 Au(111) slab. (a) Side-view, and (b) top-view. The carbene lone pair binds directionally to the slab Au atom pulling it out of the surface plane, while the large aryl substituents prevent the NHC ring from tilting towards the surface. The aryl substituents are bent upwards, displaying a nearly planar orientation relative to the surface plane (~7º).

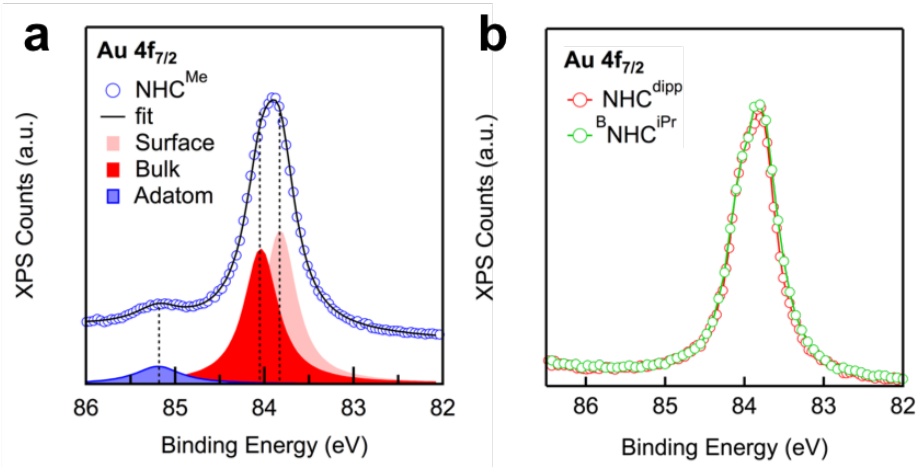

Figure S6: (a) Au $4f_{7/2}$ XPS spectrum (collected at 140 eV photon energy) for NHC^{Me} monolayer on Au(111). The XPS spectrum is fitted with three peaks using Voigt functions, corresponding to bulk (84.0 eV), surface, (83.8 eV) and adatom (85.1 eV) components. The FWHM of the surface and bulk components are set equal reported values (0.43 and 0.47 eV, respectively for bulk and surface components).[7-8] The FWHM of the adatom satellite was found to be 0.58 eV. A small linear background photoemission intensity was subtracted from the data. (b) Au $4f_{7/2}$ XPS spectra (collected at 140 eV photon energy) for $^{B}NHC^{iPr}$ (at 90 °C) and NHC^{dipp} monolayers on Au(111). No satellite peak is observed.

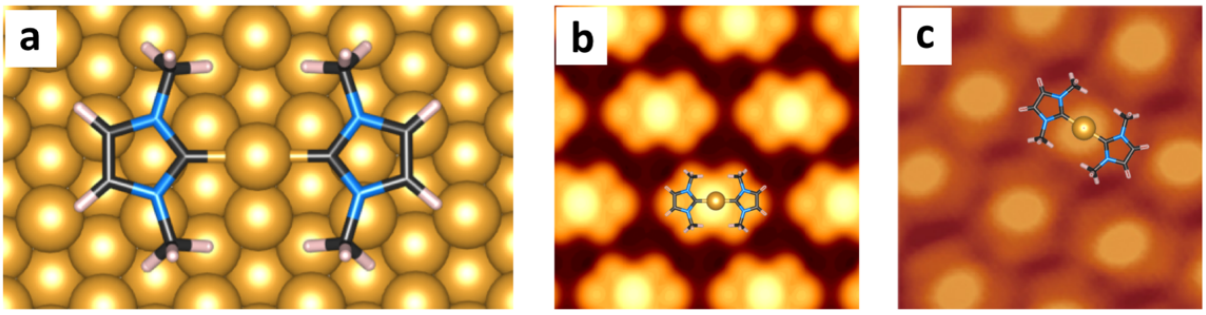

Figure S7: (a) DFT-optimized energy minimum structure of a NHC^{Me}–Au^{ad}–NHC^{Me} complex adsorbed on a 5×4 Au(111) slab. (b) Simulated constant current STM image of the NHC^{Me}–Au^{ad}–NHC^{Me} complex adsorbed on a 5×4 Au(111) slab. The simulated image was obtained by integrating the density of states up to –0.45 eV from Fermi; an isovalue of 5×10^{-8} was used to plot the 2D map. The Au adatom appears as a very bright circular spot in the center of the complex due to its high density of states near Fermi. A ball-and-stick model of the complex is overlaid on the simulated image. (c) Experimental STM image adapted from Fig. 3b in Wang *et al.*[9] The image was recorded at –0.45 V substrate bias in constant current mode (I = 15 pA). A bright circular spot appears in the center of each twofold symmetric structure whose contour closely resembles that of the simulated STM image. A ball-and-stick model of the complex is overlaid on the image. The packing of the NHC^{Me}–Au^{ad}–NHC^{Me} complex on the surface observed in (c) is not captured by the calculation presented in (b) as this would require using a much larger unit cell beyond our capabilities.

Table S1: Selected atomic distances as calculated by DFT.

	Distance (Å)	
	Au^{ad}–C	Au^{ad}-surface
NHC^{Me}	2.072	2.178
$^{B}NHC^{iPr}$	2.061	2.143
NHC^{dipp}	2.042	2.183
NHC^{Me}–Au^{ad}–NHC^{Me}	2.055	3.088
$^{B}NHC^{iPr}$–Au^{ad}–$^{B}NHC^{iPr}$	2.069	3.094

Table S2: Calculated DFT adsorption energy.

	Adsorption energy (eV)	
	On surface	On adatom
NHC^{Me}	-1.49	-2.49
$^{B}NHC^{iPr}$	-2.14	-2.85
NHC^{dipp}	-2.69	-4.11
NHC^{Me}–Au^{ad}–NHC^{Me}	-2.48	

6. References

(1) Han, Y.; Huynh, H. V.; Koh, L. L., Pd(II) complexes of a sterically bulky, benzannulated N-heterocyclic carbene and their catalytic activities in the Mizoroki–Heck reaction. *J. Organomet. Chem.* 2007, **692**, 3606-3613.

(2) Holbrey, J. D.; Reichert, W. M.; Tkatchenko, I.; Bouajila, E.; Walter, O.; Tommasi, I.; Rogers, R. D., 1,3-Dimethylimidazolium-2-carboxylate: the unexpected synthesis of an ionic liquid precursor and carbene-CO_2 adduct. *Chem. Commun.* 2003, 28-29.

(3) DeJesus, J. F.; Trujillo, M. J.; Camden, J. P.; Jenkins, D. M., N-Heterocyclic Carbenes as a Robust Platform for Surface-Enhanced Raman Spectroscopy. *J. Am. Chem. Soc.* 2018, **140**, 1247-1250.

(4) Wang, G.; Ruhling, A.; Amirjalayer, S.; Knor, M.; Ernst, J. B.; Richter, C.; Gao, H. J.; Timmer, A.; Gao, H. Y.; Doltsinis, N. L.; Glorius, F.; Fuchs, H., Ballbot-type motion of N-heterocyclic carbenes on gold surfaces. *Nature Chem.* 2017, **9**, 152-156.

(5) Stohr, J., *NEXAFS Spectroscopy*. Heidelberg: 1992.

(6) Giannozzi, P.; Baroni, S.; Bonini, N.; Calandra, M.; Car, R.; Cavazzoni, C.; Ceresoli, D.; Chiarotti, G. L.; Cococcioni, M.; Dabo, I., QUANTUM ESPRESSO: a modular and open-source software project for quantum simulations of materials. *J. Phys.: Condens. Matter* 2009, **21**, 395502.

(7) Klimes, J.; Bowler, D. R.; Michaelides, A., Chemical accuracy for the van der Waals density functional. *J. Phys.: Condens. Matter* 2010, **22**, 022201.

(8) Dion, M.; Rydberg, H.; Schroder, E.; Langreth, D. C.; Lundqvist, B. I., Van der waals density functional for general geometries (vol 92, art no 246401, 2004). *Phys. Rev. Lett.* 2005, **95**.

(9) Momma, K.; Izumi, F., VESTA 3 for three-dimensional visualization of crystal, volumetric and morphology data. *J. Appl. Crystallogr.* 2011, **44**, 1272-1276.